

**Project Title:****Prediction of Crystal Structure and Properties & Crystal Structure Prediction and High-temperature Superconductivity of Li-RE-H System at High Pressures****Name:**

Yanming MA (1), Ryotaro ARITA (1), ○Toshiaki IITAKA (2)

**Laboratory at RIKEN:**

(1) RIKEN Center for Emergent Matter Science, First-Principles Materials Science Research Team,

(2) RIKEN Center for Computational Science, Discrete Event Simulation Research Team

1. Background and purpose of the project, relationship of the project with other projects

Clathrate superhydride is a class of hydrides in which metal atoms act as guests in hydrogen (H) cages, while H atoms are weakly covalently bonded with each other and the H–H distance of approximately 1.0 Å is close to that (0.98 Å) in atomic hydrogen at 500 GPa. The first-ever sodalite-like clathrate superhydride CaH<sub>6</sub> is predicted to have high  $T_c$  values of 220–235 K at 150 GPa, which has been recently successfully synthesized by two independent experiments. Inspired by the prediction of CaH<sub>6</sub>, other compressed clathrate superhydrides, such as LaH<sub>10</sub> and YH<sub>10</sub>, are predicted to have higher  $T_c$  values at high pressure, approaching room-temperature superconductivity. Encouraged by these predictions, subsequent experiments synthesized a variety of Rare-Earth (RE) clathrate superhydrides, of which the measured  $T_c$  of YH<sub>6</sub>, YH<sub>9</sub>, and LaH<sub>10</sub> reach high values at 220, 243, and 250–260 K, respectively, setting a new record of  $T_c = 260$  K in known superconductors. These excellent theoretical and experimental effort indicates clathrate superhydrides are the most promising candidates for room-temperature superconductivity.

Nonetheless, for some clathrate superhydride, the trend of superconducting temperature with pressure in experimental is different from theoretical predictions. The experimental of CaH<sub>6</sub>, YH<sub>9</sub>, and LaH<sub>10</sub> show that their superconducting

temperatures increase first and then decrease with the increase of pressure. However, first-principles calculations indicate that their superconducting temperatures monotonically decrease with increasing pressure. To explain the potential physical mechanism from the different trends from experimental and calculation, we conducted a study using CaH<sub>6</sub> as an example.

Here we reports a comprehensive exploration of the potential physical mechanisms represented by the trend of superconducting temperature changes with pressure for clathrate superhydrides, represented by CaH<sub>6</sub>. In this work, a structure prediction was conducted for CaH<sub>6</sub> in 100 GPa and 135 GPa. The results show that in addition to the previously predicted  $Im\bar{3}m$  superconducting phase, there are other low-enthalpy, low-symmetry phases that may be stable at low pressures, such as  $P2$  phase,  $P\bar{3}$  phase and  $R\bar{3}m$  phase. We analyzed this low-symmetry phases that may be stable at low pressures and conducted an analysis of their superconducting properties. At the same time, we calculated the Ca-H clathrate superhydrides with different H contents at 135 GPa and 150 GPa such as Ca<sub>8</sub>H<sub>46</sub> and CaH<sub>6</sub> defects structure with special H cages. We calculated Ca<sub>16</sub>H<sub>92</sub> and Ca<sub>16</sub>H<sub>94</sub> with chemical ratios of Ca:H = 1:5.75 and Ca:H = 1:5.875, respectively. We explored all combinations of H atom vacancies and sorted the possible structures by electrostatic energy, and studied the superconducting properties of the top 20 structures with the lowest energy. At the same time, we

analyzed the impact of quantum non-harmonic effects on the thermodynamic stability and superconducting temperature of Ca-H Clathrate superhydrides under different pressures. Among these results, we found that after considering quantum and anharmonic effects, low-symmetry phases that are stable at low pressures will all be optimized to  $Im\bar{3}m$  phase. The average electronic state density of defects structure with different H contents,  $\text{Ca}_{16}\text{H}_{92}$  and  $\text{Ca}_{16}\text{H}_{94}$ , shows the same trend as the experiment.

## 2. Specific usage status of the system and calculation method

During the fiscal year 2023, 2.4 million CPU hours were used to investigate the superconducting mechanism of clathrate superhydrides with high superconducting temperatures. We employ our developed swarm-intelligence-based CALYPSO structure prediction method, which is designed to search for the stable structures of given compounds, for the investigation of phase stability of CaH6 compounds at 100 GPa and 135 GPa. For most cases, the structure search for each chemical composition converges (evidenced by a lack of any additional structure with lower energy) after 1000 ~ 1200 structures were investigated.

The underlying energetic calculations are performed with the plane-wave pseudopotential method as implemented in the VASP code. The Perdew-Burke-Ernzerhof generalized gradient approximation is chosen for the exchange-correlation functional. The electron-ion interaction is described by projector-augmented-wave potentials with 1 and 10 valence electrons for H, and Ca atoms, respectively. Kinetic cutoff energy of 700 eV and Monkhorst-Pack k meshes with a grid spacing of  $0.25 \text{ \AA}^{-1}$  are adopted to ensure the enthalpy converges to better than 1 meV/atom.

The phonon spectrum and electron-phonon coupling (EPC) of the stable compounds are calculated within the framework of linear response theory through the Quantum-ESPRESSO code, where ultrasoft pseudopotentials were used with a kinetic energy cutoff for wavefunctions of 80 Ry and a kinetic energy cutoff for charge density and potential of 640 Ry.  $12 \times 12 \times 12$  q-meshes and  $12 \times 12 \times 12$  k-meshes were used for CaH6 to compute the EPC matrix elements. Electron-phonon couplings (EPC) constant  $\lambda$ ,  $\omega_{\text{log}}$ , and  $T_c$  are solved using the elk code, as derived by the direct solution of the isotropic Migdal-Eliashberg equation.

Phonon spectra and superconducting transition temperature in anharmonic level based on the variational stochastic self-consistent harmonic approximation (SSCHA) method. The SSCHA calculations were performed using a  $2 \times 2 \times 2$  supercell, yielding dynamical matrices on a commensurate  $2 \times 2 \times 2$  q-point grid in Brillouin zone (BZ). The total energies, forces, and stress tensors for the individuals are obtained from DFT calculations. At the end of a minimization run, a new population with higher number of individuals N is generated from the minimized trial density matrix until convergence. In calculations based on DFT we increased N up to 1000 individuals. The total forces in the last population are well below  $10^{-6} \text{ meV/\text{Å}}$ . For CaH6, The difference between the harmonic and anharmonic dynamical matrices in the  $2 \times 2 \times 2$  q-point grid was interpolated to a  $12 \times 12 \times 12$  grid. Adding the harmonic  $2 \times 2 \times 2$  grid dynamical matrices to the result, the anharmonic  $12 \times 12 \times 12$  q-grid dynamical matrices were obtained. Then a  $24 \times 24 \times 24$  k-point grid and a  $12 \times 12 \times 12$  q-point grid were used for the anharmonic EPC calculation.

## 3. Result

Due to the high concentration of Hydrogen (H) in CaH<sub>6</sub>, and considering that Hydrogen is the lightest element in the periodic table, the vibrational modes of its atomic nuclei are complex. Harmonic approximation, which only considers second-order phonon scattering, may not be sufficient to accurately describe the true ionic vibrational behavior of this compound. Therefore, in order to investigate the underlying physical mechanism of the superconducting temperature of CaH<sub>6</sub> as a function of pressure, we have considered the impact of quantum and anharmonic effects on the phonon spectrum (Fig. 1) and superconducting temperature of CaH<sub>6</sub> (Fig. 2). We found that while quantum anharmonic effects did not alter the trend of CaH<sub>6</sub>'s superconducting temperature as a function of pressure, they strongly suppressed phonon softening, thereby reducing the  $T_c$  of CaH<sub>6</sub>.

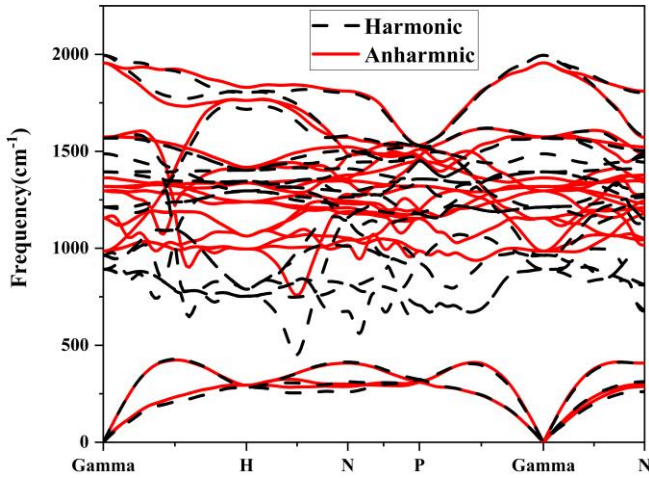


Fig 1. Comparison between the anharmonic (red solid line) and harmonic (black dash line) phonon spectra of CaH<sub>6</sub> at 165 GPa.

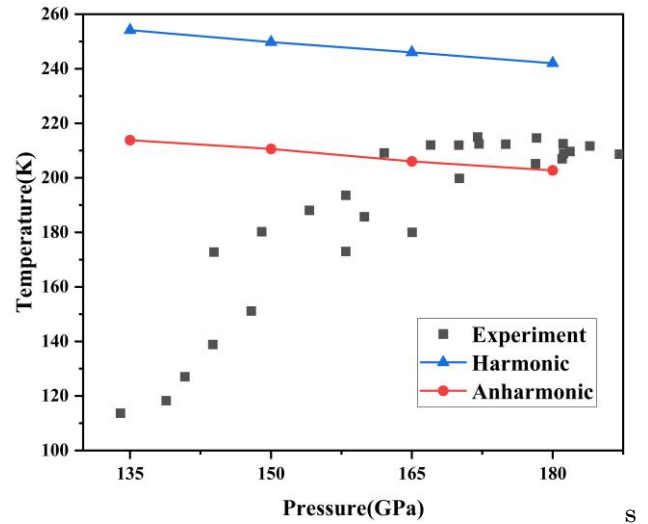


Fig 2. The superconducting transition temperatures of *Im-3m*-CaH<sub>6</sub>. The red circle were calculated using harmonic approximation and the blue triangle were calculated by introducing an anharmonic effect. the Coulomb shielding pseudopotential  $\mu^*$  is set to be 0.10.

Subsequently, we conducted structural predictions for CaH<sub>6</sub> at pressures of 100 GPa and 135 GPa. We have discovered some low symmetry phases that may exist stably under low pressure, such as *P-3* phase, *R-3m* phase, etc (Fig. 3). In the pressure range of 135 - 150 GPa, only the enthalpy value of *P-3* phase is lower than that of CaH<sub>6</sub>, and the superconducting transition temperature at 150 GPa is 129 K, which is lower than the superconducting temperature of CaH<sub>6</sub> at 150 GPa at 210 K, consistent with the experimental result. However, when considering the quantum anharmonic effect, the *P-3* phase of CaH<sub>6</sub> will be symmetrized into the *Im-3m* phase.

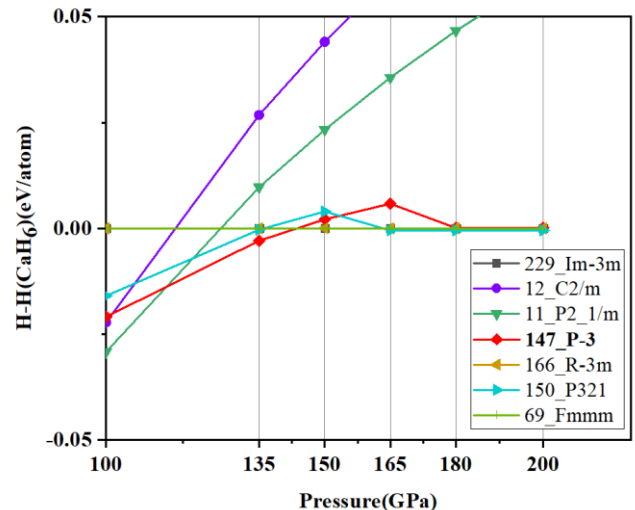


Fig 3. The enthalpy difference between CaH<sub>6</sub> low symmetric phase and CaH<sub>6</sub> *Im-3m* phase at different pressures.

Since Ba<sub>8</sub>H<sub>46</sub> and Eu<sub>8</sub>H<sub>46</sub> have been synthesized in experiments, we replace the metal cation in it with Ca and build Ca<sub>8</sub>H<sub>46</sub>. Under the harmonic approximation, Ca<sub>8</sub>H<sub>46</sub> in 200GPa is dynamics stable. After considering the quantum and anharmonic effect, Ca<sub>8</sub>H<sub>46</sub> exhibits dynamic stability at 150 GPa. The superconducting temperature of Ca<sub>8</sub>H<sub>46</sub> at 200 GPa decreased from 208 K to 185 K, and at 150 GPa it was 215 K. Under the quantum and anharmonic effect, the superconducting temperature of Ca<sub>8</sub>H<sub>46</sub> still shows a decreasing trend with pressure.

Due to the difficulties in locating hydrogen in x-ray diffraction (XRD) measurements, clathrate hydrides usually have undetermined hydrogen positions. In experiments, the hydrogen positions are set in the interstitial sites of the host lattice, together with the number of hydrogen atoms counted from the volume difference between hydrides and pure metal. In this way, experimental studies generally report imperfect stoichiometries, e.g., LaH<sub>9.6</sub> and CeH<sub>9.8</sub>. However, in experiment-simulation combined studies, the position and number of hydrogen atoms are generally inferred based on comparison between the experimental equation of states (EoS) measured at room temperature and the theoretical EoSs calculated for ideal crystals at zero temperature. So we consider that structures in the range of 135 GPa to 165 GPa where the superconducting temperature increases with pressure may contain stoichiometric defects.

By randomly removing 2 H atoms and sorting the possible structures by electrostatic energy, we constructed Ca<sub>16</sub>H<sub>94</sub> structures containing defects from the top 20. The average density of states of these structures shows a consistent trend with the variation of superconducting temperature in CaH<sub>6</sub>

experiments as a function of pressure, with an initial increase followed by a decrease. These structures are dynamically unstable under harmonic approximation. We took one of them, Ca<sub>16</sub>H<sub>94</sub>-*Ama2*, and calculated the superconducting temperature at 150 GPa, taking into account the anharmonic effect.

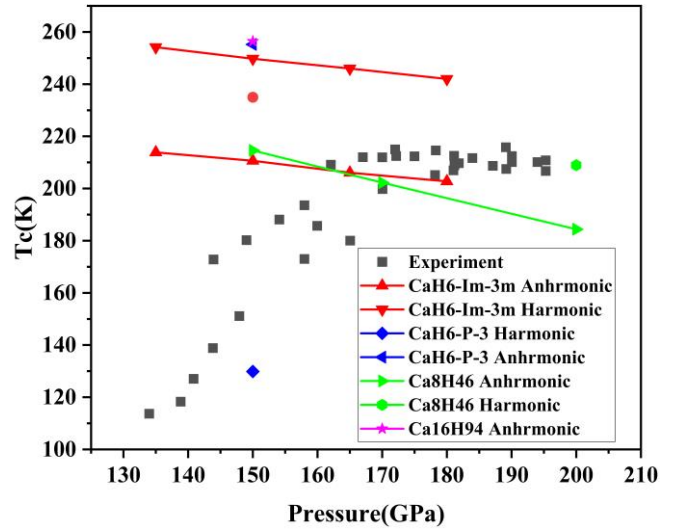


Fig 4. The superconducting transition temperatures. The Coulomb shielding pseudopotential  $\mu^*$  is set to be 0.10.

#### 4. Conclusion

In summary, by considering possible low pressure phases, different Ca-H chemical ratios, we add a quantum and anharmonious effect, we studied the superconducting temperature of CaH<sub>6</sub> as a function of pressure. The low-pressure phase P-3 of CaH<sub>6</sub> is 125 K at 150 GPa, which is much lower than that of CaH<sub>6</sub> *Im-3m* phase. Its superconducting transition temperature at 150 GPa is 210 K. However, considering the quantum and anharmonic effect will transform all low symmetry phases into *Im-3m* phases. The superconducting temperature of structures with less H content is equivalent to that of CaH<sub>6</sub>. Our results indicate that the quantum anharmonic effect tends to optimize the structure to have higher symmetry, and the possible H atom defects in the CaH<sub>6</sub> experiment are not the reason for the first increase and then decrease of the superconducting temperature curve with pressure.

## Usage Report for Fiscal Year 2023

The decrease in superconducting temperature during the unloading process of the sample may have deeper physical mechanisms. Our results indicate that the quantum anharmonic effect tends to optimize the structure to have higher symmetry, and the possible H atom defects in the CaH<sub>6</sub> experiment are not the reason for the first increase and then decrease of the superconducting temperature curve with pressure. The decrease in superconducting temperature during the unloading process of the sample may have deeper physical mechanisms.

### 5. Schedule and prospect for the future

I have been a HOKUSAI general user and wish to continue using the system. During the last fiscal year 2023, I have finished work on Ca-H compounds. For the next fiscal year, we plan to continue using the HOKUSAI supercomputer to study the stability and superconductivity of compressed superhydrides, where new high-temperature superconductors and even room-temperature superconductors are expected to be proposed. We expect high-standard publications can be eventually achieved.

### 6. If no job was executed, specify the reason.

Usage Report for Fiscal Year 2023

**Fiscal Year 2023 List of Publications Resulting from the Use of the supercomputer**